Geophysical Research Letters

RESEARCH LETTER
10.1029/2021GL094307

Special Section:
The Arctic: An AGU Joint Special Collection

Liquid Containing Clouds at the North Slope of Alaska Demonstrate Sensitivity to Local Industrial Aerosol Emissions

Maximilian Maahn[1], Tom Goren[1], Matthew D. Shupe[2,3], and Gijs de Boer[2,3,4]

[1]Leipzig University, Leipzig Institute for Meteorology, Leipzig, Germany, [2]University of Colorado, Cooperative Institute for Research in Environmental Sciences, Boulder, CO, USA, [3]NOAA Physical Sciences Laboratory, Boulder, CO, USA, [4]University of Colorado, Integrated Remote and In Situ Sensing, Boulder, CO, USA

Key Points:

- Localized pollution reduces cloud droplet size in the Prudhoe Bay region
- The reduced droplet size increases cloud-reflected shortwave radiation up to 0.8 W/m^2
- Strong regional gradients prohibit an analysis of pollution impact on cloud frequency or liquid water content

Supporting Information:

Supporting Information may be found in the online version of this article.

Correspondence to:

M. Maahn,
maximilian.maahn@uni-leipzig.de

Citation:

Maahn, M., Goren, T., Shupe, M. D., & de Boer, G. (2021). Liquid containing clouds at the North Slope of Alaska demonstrate sensitivity to local industrial aerosol emissions. *Geophysical Research Letters*, *48*, e2021GL094307. https://doi.org/10.1029/2021GL094307

Received 11 MAY 2021
Accepted 10 AUG 2021

Abstract Cloud condensation nucleus control alter cloud solar albedo through cloud droplet size. Here, we leverage anthropogenic emissions at the North Slope of Alaska as a natural laboratory to study relationships between aerosols and Arctic liquid-containing clouds. Averaging 14 years of MODIS observations, we found a reduction in temporally averaged cloud effective radius (r_e) of up to 1.0 μm related to localized pollution. Pronounced regional gradients in cloud frequency of occurrence and liquid water path prohibit the detection of potential changes of these variables. Observed changes of r_e alter radiative fluxes and increase cloud-reflected shortwave radiation by up to 0.8 W m^{-2} in the Prudhoe Bay area for the period covered by observations (April–September). Due to the frequent occurrence of liquid-containing clouds, this implies that enhanced local emissions in Arctic regions can impact climate processes.

Plain Language Summary The interactions between aerosols and clouds are still not fully understood despite their importance for the Earth's weather and climate. Cloud condensation nuclei (CCN) are a type of aerosol particles that control cloud droplet size and the brightness of clouds. Their impact on other cloud properties is unclear. Here, we leverage industrial emissions at the North Slope of Alaska as a natural laboratory to study relationships between aerosols and Arctic liquid containing clouds. We found a notable reduction in cloud droplet size, but strong local gradients prohibit quantifying an impact on other cloud properties. The change in cloud droplet size is sufficient to make the clouds brighter. Because the frequent occurrence of liquid-containing clouds in the Arctic, this shows a potential impact of local industrial emissions on climate processes.

1. Introduction

Clouds significantly influence the global climate system, notably impacting the surface energy and mass balances through radiative and precipitation processes (Stephens, 2005). Aerosol perturbations alter cloud microphysics through indirect and semidirect effects. For example, increased cloud condensation nucleus (CCN) concentrations result in elevated cloud droplet concentrations (N_l). If total condensate mass does not change, increased N_l results in decreased cloud droplet size, enhancing cloud albedo (Quaas et al., 2020; Twomey, 1976) and longwave emissivity for optically thin clouds (Garrett & Zhao, 2006; Lubin & Vogelmann, 2006). Aerosols may also impact cloud lifetime through alteration of precipitation processes (Albrecht, 1989), though recent studies (Gryspeerdt et al., 2019; Malavelle et al., 2017; Rosenfeld et al., 2019; Toll et al., 2019; Trofimov et al., 2020; Wood, 2007) show limited relationships between liquid water path (LWP) and aerosol concentration, suggesting system buffering (Stevens & Feingold, 2009). Challenges associated with quantifying these aerosol-cloud effects contribute significantly to uncertainties in understanding the climate system, in particular in the Arctic (Engelmann et al., 2020; Schmale et al., 2021; Zamora et al., 2018).

At high latitudes, frequent occurrence of mixed-phase clouds (de Boer et al., 2009; Shupe, 2011; Shupe et al., 2005) further complicates aerosol-cloud relationships (Korolev et al., 2017). Ice in these clouds acts as a cloud water sink (Morrison et al., 2012), and increased ice nucleating particle (INP) concentrations reduce cloud liquid water through the Wegener-Bergereon-Findeisen process (Korolev, 2007). This effect and the challenges associated with correct representation of ice microphysics in models wreak havoc on simulation of mixed-phase clouds (Klein et al., 2009; Lohmann, 2002; Morrison et al., 2005; Sulia & Harrington, 2011;

Yang et al., 2015). Simultaneously, liquid droplet characteristics affect ice crystal properties through precipitation process such as riming (e.g., Borys et al., 2003; Hallett & Mossop, 1974), meaning CCN concentrations also influence precipitation, cloud lifetime and radiative effects (Norgren et al., 2018). The presence of liquid water may even be a prerequisite for ice formation at moderate temperatures (de Boer et al., 2011), and increased concentrations of large drop sizes have been associated with ice production (Lance et al., 2011; Rangno & Hobbs, 2001). Recent modeling work to untangle these competing effects concluded that INP perturbations dominate proportional increases in CCN (Solomon et al., 2018).

Statistical analysis across the seasonal cycle of Arctic aerosol properties provides opportunities for understanding key relationships (Coopman et al., 2018; Garrett & Zhao, 2006; Zamora et al., 2017) but the quantification of aerosol influences on clouds is additionally muddied by the conflation of these effects with meteorological drivers (i.e., changes in moisture content and dynamics, Feingold et al., 2016; Gryspeerdt et al., 2016; Rosenfeld et al., 2019; Sena et al., 2016). To circumvent this issue, Arctic ship emissions are used as a natural laboratory (Gilgen et al., 2018; Possner et al., 2017), but are limited in extent and occurrence.

In this study, the natural laboratory concept is expanded by investigating aerosol influences on clouds using surface- and satellite-based observations from Northern Alaska. Petroleum extraction in and around the Prudhoe Bay Oilfield has resulted in continuous release of anthropogenic emissions over the past several decades with anthropogenic sulfur dioxide emissions of 17.37 kt/year (Klimont et al., 2017). These rates are similar to those observed at mid-latitudes, even though only a small area is impacted at the North Slope of Alaska (Figure 1). Localized aerosol gradients from these emissions have been observed by research aircraft (Creamean et al., 2018) and linked to increased N_l (Hobbs & Rangno, 1998) and reduced r_e (Maahn et al., 2017). In combination with decreased aerosol transport from lower latitudes (Quinn et al., 2009), the role of local emissions in controlling cloud properties could be increased due to higher susceptibility of cleaner clouds (Platnick & Twomey, 1994). In addition to localized aerosol sources, the North Slope of Alaska features flat terrain and limited spatial variability in meteorology: surface measurements of temperature, humidity, and surface pressure at Oliktok Point and Utqiaġvik (formerly Barrow) are correlating at 0.96, 0.95, and 0.97, respectively, according to data recorded at the Department of Energy Atmospheric Radiation Measurement (DOE ARM) sites (Holdridge & Kyrouac, 1993). For Utqiaġvik, Sedlar et al. (2021) found that cloud formation and dissipation is mostly controlled by synoptic events. This results in a favorable setting with limited confounding factors (Grandey & Wang, 2019; Sena et al., 2016) in which to evaluate aerosol-cloud interactions. Leveraging two decades of observations, we demonstrate statistically significant aerosol-based modification of cloud properties over the Prudhoe Bay Oilfield, similar to the case shown in Figure 2 where—in comparison to adjacent areas—more overcast clouds, increased cloud brightness, and decreased cloud r_e are seen.

2. Data and Methods

We analyzed MODIS (Moderate Resolution Imaging Spectroradiometer) swaths collected between 04/2006 and 12/2019 from the Terra and Aqua satellite cloud products (MOD06L2, MYD06L2, collection 6, Platnick & Ackerman, 2015a; Platnick & Ackerman, 2015b). The MODIS products were nearest-neighbor gridded to a 2 km resolution, which greatly expands the data set in comparison to the published MODIS cloud products with daily resolution because multiple daily overpasses are available at high latitudes. To quantify the impact of localized emissions, we selected a Prudhoe Bay region for further analysis that includes almost all oil wells and is slightly extended downwinds (insert Figure 1, orange box) in accordance with the predominant wind direction being from the East (see wind rose in Figure 1). To allow comparisons, we selected a reference region between Utqiaġvik and Prudhoe Bay with similar properties with respect to the number of land pixels, proximity to the ocean, and elevation (insert Figure 1, green box).

To minimize contamination in connection with known deficiencies in the retrieval algorithm, only those 14,755 overpasses were analyzed that feature satellite viewing zenith angles (VZA) less than 56° (Maddux et al., 2010) and solar zenith angles (SZA) less than 65° (Grosvenor & Wood, 2014; Khanal et al., 2020) with

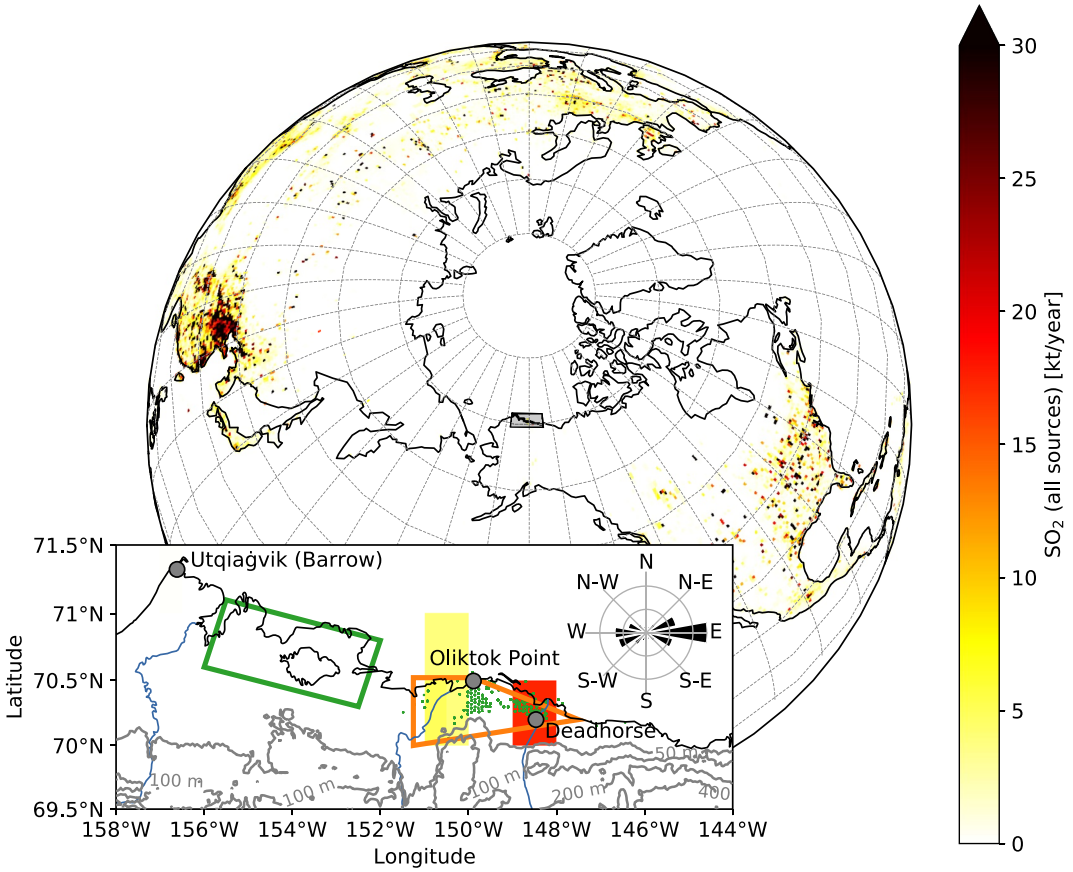

Figure 1. Yearly sulfur dioxide emissions based on an inventory by Klimont et al. (2017) for the northern hemisphere and the study region (insert). The insert shows also isolines for height above sea level (gray) and a wind rose for the 925 hPa level based on ERA5. The green dots correspond to oil wells active in March 2017, the green and orange boxes indicate the the reference region and the Prudhoe Bay region, respectively.

the latter limiting the investigated time period to April–September. Also, cloud observations with small optical thickness (τ) are know to be unreliable (Goren et al., 2018; Sourdeval et al., 2015) and only clouds with τ greater than five were included in the analysis. Additionally, the MODIS single layer flag is used to remove multi layer clouds to attempt to limit analyzed clouds to those impacted by localized pollution. This analysis focuses on the liquid-containing clouds as identified by the MODIS cloud phase flag. This removes only 4%–7% of the clouds in our data set (see Text S1), because most ice clouds are already removed by the optical thickness threshold. Due to deficiencies of the standard MODIS retrieval for identifying clouds over bright surfaces, the standard retrieval is only applied to pixels without surface snow (based on the National Ice Center's Interactive Multisensor Snow and Ice Mapping System (IMS) Daily Northern Hemisphere Snow and Ice Analysis at 4 km Resolution, Ramsay, 1998; Helfrich et al., 2007; National Ice Center, 2008, updated daily) and a retrieval developed for use over bright surfaces using the 1.6 and 2.1 μm channels (Platnick et al., 2001) is applied otherwise. Our analysis is limited to clouds occurring in pixels over land surfaces only due to the potential impacts of inhomogeneous sea ice surfaces on cloud property retrievals. Pixels containing ocean or lakes were removed to ensure homogeneous surface properties. Also data with surface elevation higher than 100 m above sea level has been removed to minimize interference from orographic lifting processes.

From the MODIS products, cloud liquid droplet effective radius (r_e) and liquid water path (LWP) were used for further analysis. Cloud frequency of occurrence (CFO) is estimated by the ratio of pixels with identified clouds (i.e., $\tau \geq 5$) to the number of total observations after removal of data with too large SZA or VZA as

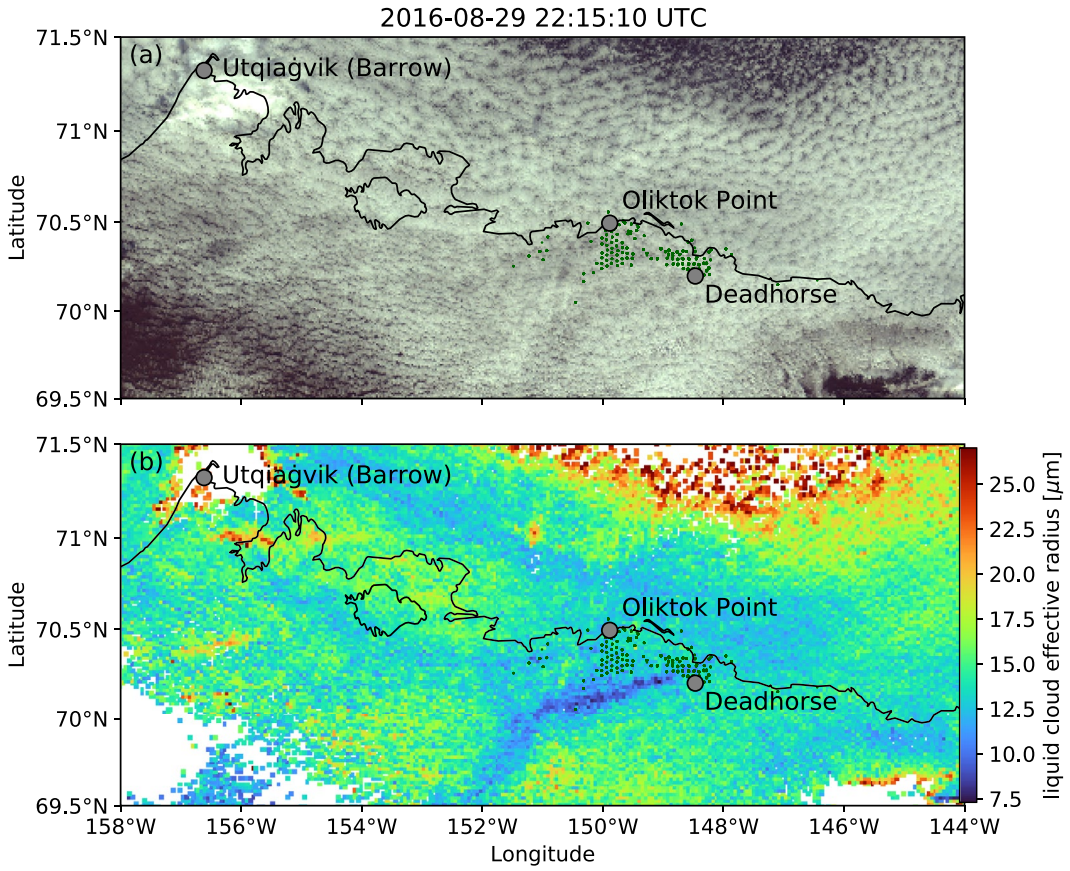

Figure 2. Case study showing the impact of local emissions on cloud properties. (a) Terra Moderate Resolution Imaging Spectroradiometer (MODIS) true color image and (b) MODIS liquid cloud effective radius (r_e) retrieval on 2016-08-29 at 22:15:10 UTC with clear areas indicating areas without liquid clouds. Black lines show shorelines and dark green dots mark oil wells. The case shows a change in cloud brightens and r_e downwind of the eastern part of the Prudhoe Bay region where the emission inventory reports the highest sulfur dioxide emissions (Figure 1). For this case, ERA5 925 hPa wind direction at Oliktok Point was 95°.

discussed above. Only data points with identified clouds are considered when calculating mean r_e and mean LWP. A potential change in upwelling shortwave radiation ($\Delta SW_{\uparrow}$) is estimated from the difference in albedo $\Delta\alpha_C$ combined with the downwelling shortwave radiation at the surface ($SW_{\downarrow}$) and the appropriate CFO (Charlson et al., 1992; Meskhidze & Nenes, 2006):

$$\Delta SW_{\uparrow} = SW_{\downarrow} \times CFO \times \Delta\alpha_C \tag{1}$$

here, $SW_{\downarrow}$ is derived from monthly clouds and the Earth's Radiant Energy System (CERES) observations on Terra. Monthly values for liquid cloud frequency CFO are estimated using the criteria outlined above except the single layer filter, because the goal is to asses the mean impact on radiation for all cloud conditions. We assume that clouds are adiabatic with vertically constant droplet number concentrations and estimate the monthly averaged $\Delta\alpha_C$ with (McCoy & Hartmann, 2015)

$$\Delta\alpha_C = \frac{1}{3}\alpha_C \times (1-\alpha_C) \times \left[1 - \frac{r_e^3}{r_{e,\text{reference}}^3}\right] \tag{2}$$

where we use monthly pixel mean values for r_e and spatially averaged monthly mean values for $r_{e,\text{reference}}$ based on the reference region. α_C is estimated from monthly averaged MODIS τ with

$$\alpha_C = \frac{0.13 \times \tau}{1 + (0.13 \times \tau)} \tag{3}$$

following Lacis and Hansen (1974). The estimated mean $\Delta SW_{\uparrow}$ value is only applicable to the six months season covered by the observations (April–September). Assuming that $\Delta SW_{\uparrow}$ for winter months without observations is 0 $W m^{-2}$, the $\Delta SW_{\uparrow}$ value representative for the full year would be reduced by 50%.

3. Results

Figure 3a shows how the mean cloud liquid droplet effective radius (r_e) is reduced in the Prudhoe Bay region in comparison to the reference area. The reduction of r_e is not homogeneous in the Prudhoe Bay region and is strongest in the eastern part (up to 1.0 μm). The area with reduced r_e expands about 100 km down-wind in accordance with the predominant Easterly wind direction. This is consistent with the location of the largest sulfur dioxide emissions according to the inventory (insert Figure 1). Because surface elevation in the area with reduced r_e is below 50 m (insert Figure 1), we assume that the impact of lifting processes on these signatures can be neglected. Characterizing the spatial variability of r_e change, the first and fifth percentiles of the 970 pixel in the Prudhoe Bay region are reduced 0.78 μm and 0.60 μm, respectively, but it should be noted that these values depend also on the boundaries used for the Prudhoe Bay region. The relatively small r_e reduction is explained by the fact that the data is temporally averaged over all cases and a variety of cloud types and background aerosol concentrations. For individual cases, the r_e reduction can be substantially larger as illustrated in Figure 2b.

To account for r_e changes of individual cases, we also compared distributions of all MODIS cloud observations within the two regions, that is, temporal averaging is not applied (insert Figure 3a). For the Prudhoe Bay region, we find that the median r_e is significantly (5% confidence interval, Mood's t-test) reduced by 0.28 μm in comparison to the reference region. The comparison of the distributions of individual cases reveals that the r_e reduction in the Prudhoe Bay region is stronger for the 75th percentile (0.44 μm difference between both regions) than for the 25th percentile (0.21 μm difference). This shows the higher susceptibility of rather pristine clouds with larger r_e values with respect to changes related to localized pollution (Platnick & Twomey, 1994). Our results for r_e are robust with respect to the chosen filtering and channel combination as shown in Text S2.

When limiting the analysis to times for which winds aligned with the predominant wind direction (60°–110°, 36% of the total cases based on the fifth generation ECMWF atmospheric reanalyzes (ERA5) with 30 km resolution (Copernicus Climate Change Service (C3S) 2017) at the 925 hPa level), the detected temporal mean r_e reduction becomes larger (up to 1.35 μm, Figure 3b) and the median of the distribution of all cloud observation is reduced by 0.41 μm. Spatially, the plume extends more than 200 km to 153° W Longitude which corresponds to approximately 8 h of airmass lateral advection considering the ERA5 median 925 hPa wind speed of 7 ms^{-1}—consistent to the time scales reported by Gryspeerdt et al. (2021) for ship tracks. The plume generally does not extend to Utqiaġvik, even though it has been found that aerosol properties at Utqiaġvik are impacted by localized pollution 8% of the time (Kolesar et al., 2017).

To further support our hypothesis that observed changes of r_e are connected to emissions from the Prudhoe Bay region, we leverage MODIS' cloud top pressure (CTP) retrieval to subdivide the data set. This is done with the assumption that local emissions should more directly impact lower clouds than higher clouds, particularly given the stratified nature of the Arctic atmosphere. We assume that lower clouds, those with CTP ≥ 750 hPa (Figure 3c), have on average also lower cloud bases making them more susceptible for localized pollution effects. Indeed, low clouds show more pronounced reductions in r_e around the Prudhoe Bay area (r_e reduction up to 1.13 μm) than observed for the complete data set (Figure 3a).

To assess whether these changes in cloud microphysics alter cloud lifetime, we evaluated spatial patterns of cloud frequency of occurrence (CFO) from MODIS (Figure 4a). In the eastern part of the Prudhoe Bay region with largest sulfur dioxide emissions, individual pixels shows CFO values increased by 1–2 percentage points in comparison to the remaining Prudhoe Bay region. But it is unclear whether these are random effects, because potential signals related to localized pollution are overlayed by an 8 percentage point meridional CFO gradient that is observed for the whole study region. We are confident that the meridional gradient is not caused by an instrument artifact related to a change of mean VZA within the study area, because we removed data at high VZA and the remaining spatial variability of mean VZA is only 1.5°. Also, mean liquid water path (LWP, Figure 4b) of the identified liquid containing clouds shows a pronounced

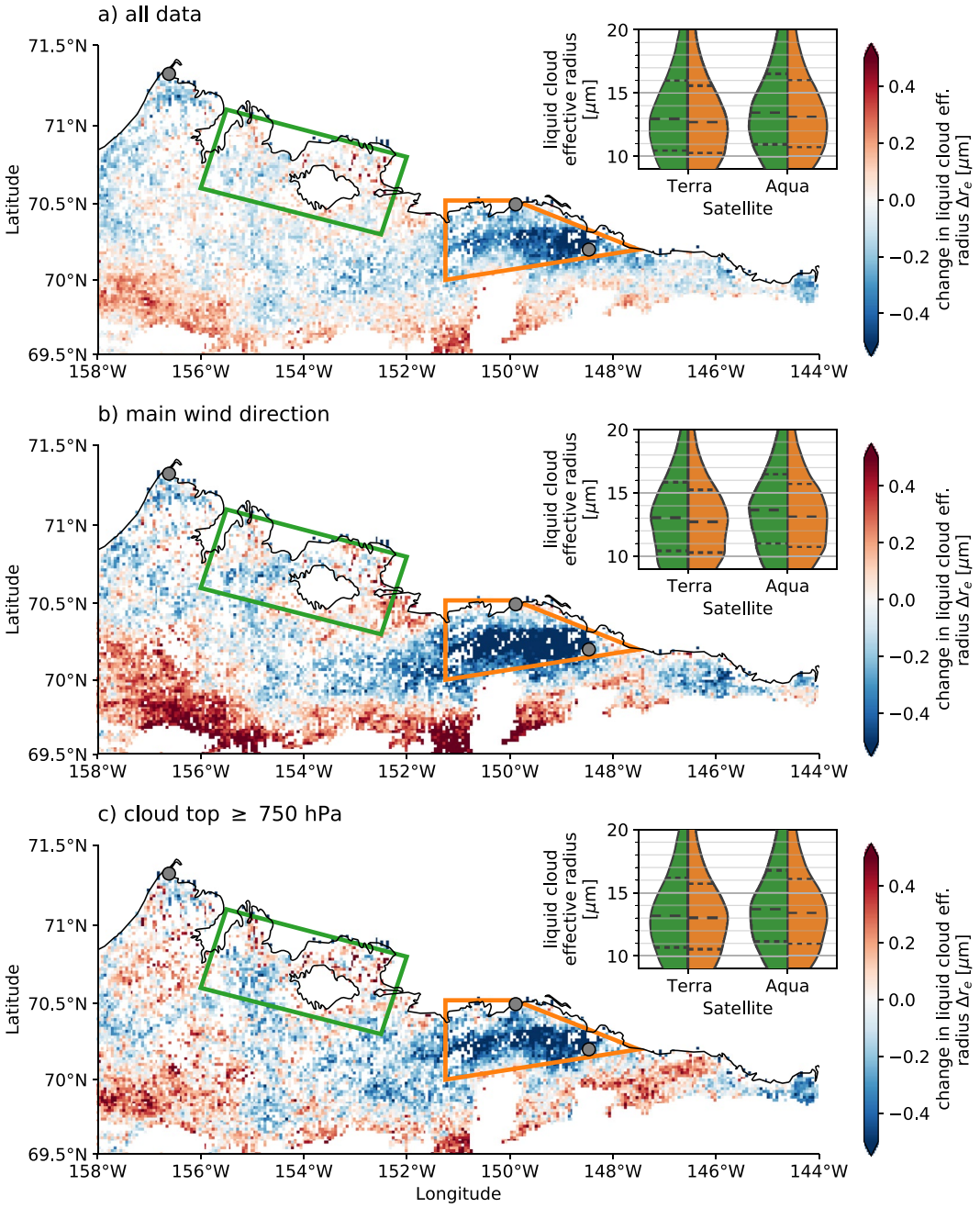

Figure 3. (a) Spatial deviation of Moderate Resolution Imaging Spectroradiometer (MODIS) mean liquid cloud effective radius r_e in comparison to a reference region (green quadrangle). The MODIS standard retrieval is used during periods without snow on the ground while the 1.6/2.1 μm retrieval is used for periods with snow cover. The normalized r_e distributions for all observations in the Prudhoe Bay region (orange quadrangle) and the reference region are shown in the insert with the lines representing the median as well as the 25th and 75th percentiles. The gray circles indicate (from left to right) Utqiaġvik, Oliktok Point, and Deadhorse; black lines show shorelines. (b) as (a), but limited to the main wind direction defined as 60°–110° from ERA5 at 925 hPa at Oliktok Point. (c) as (a), but limited to clouds with MODIS' cloud top pressure larger than 750 hPa. The medians of the distributions of the two regions are significantly different (5% confidence interval) for all three data sets.

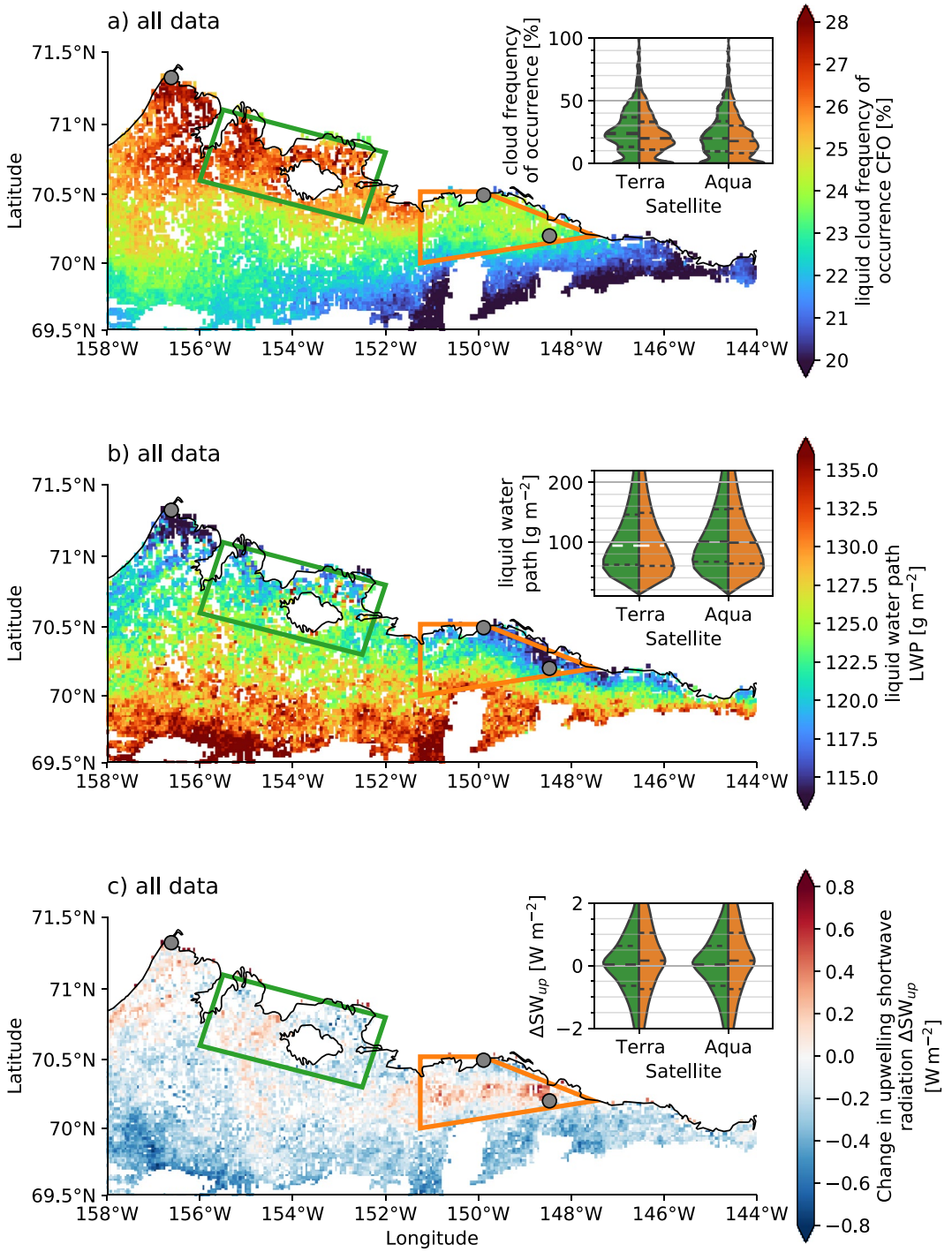

Figure 4. Spatial patterns of Moderate Resolution Imaging Spectroradiometer (MODIS) products showing (a) liquid containing cloud frequency of occurrence (CFO), (b) mean liquid water path (LWP), and (c) change in shortwave upwelling radiation $\Delta SW_{\uparrow}$ with respect to the reference region (green box). The embedded violin plots show the underlying normalized distributions for the study (orange) and reference (green) region with the lines representing the median as well as the 25th and 75th percentiles. Note that for CFO and $\Delta SW_{\uparrow}$, the distribution of monthly values is shown and the full (i.e., non averaged) data set is shown for LWP. Median values colored in black indicate a significant difference (5% confidence interval) between the medians of the two regions. The gray circles indicate (from left to right) Utqiaġvik, Oliktok Point, and Deadhorse; black lines show shorelines.

LWP difference of 20 g m^{-2} between the pixels located close to the shore and in the southern parts of the study area. Contrasting to the meridional gradient for CFO, this gradient appears to be perpendicular to the coastline so that mean LWP values are almost identical for both regions. The coastal LWP gradient correlates with the orography (insert Figure 1) so that a connection to lifting processes seems a possible explanation. No LWP patterns are visible within the Prudhoe Bay region that are consistent with the location of the strongest emissions. The strong regional gradients imply that we cannot asses whether there is an impact of localized emissions on CFO or LWP. However, our data allows to define an upper threshold for such effects. If there was a change in LWP and CFO, it must be smaller than the large scale variability observed within the Prudhoe Bay region. This indicates an upper limit for CFO and LWP changes related to localized emissions of approximately 2 percentage points and 5 g , respectively^{-2}m.

Ultimately, any aerosol-induced changes to cloud micro- and macrophysical properties are important because of their combined impact on the Earth's energy budget. It is estimated that the decrease of r_e leads to a mean enhancement of 0.03 Wm^{-2} of $\Delta SW_{\uparrow}$ for the Prudhoe Bay region during the observation period (April–September). The enhancement is not distributed homogeneously and individual pixels reach 0.79 Wm^{-2}; the first and fifth percentiles are 0.53 Wm^{-2} and 0.37 Wm^{-2}, respectively (Figure 4c). The distributions of monthly averaged $\Delta SW_{\uparrow}$ values also indicate the spatial variability with the 75th percentile featuring a larger change than the medians (see insert Figure 4c). The southern parts of the study area show a mean $\Delta SW_{\uparrow}$ of −0.4 to −0.2 Wm^{-2} which is related to increased r_e values in this region (Figure 3). The $SW_{\uparrow}$ enhancement in the Prudhoe Bay region reduces radiation arriving at the surface, thereby resulting in a net cooling of the surface environment. However, this relatively small cooling could be further modulated by small changes in CFO below our detection threshold (e.g., 1 percentage points). Such changes would if positive, for all but peak summer months, result in a compensating effect to the aerosol cloud interaction influence on net radiative forcing, taking into account the typical longwave forcing of liquid-containing Arctic clouds, which can be up to 65 Wm^{-2} (Shupe & Intrieri, 2004). The current analysis does not support the presence of any pollution-induced CFO change. This makes it challenging to come to firm conclusions about the ability of local sources of aerosol particles to drive CFO changes, and to determine if such eventual changes would compensate or enhance changes of $\Delta SW_{\uparrow}$.

4. Discussion

To evaluate the impact of anthropogenic aerosol particles on Arctic clouds an extended (14 years) time series of MODIS observations consisting of 14,755 overpasses during the polar day was analyzed. To our knowledge, the current study represents the first attempt to constrain the impact of anthropogenic emissions on clouds existing in the clean Arctic background state using "natural laboratory" observations over a long time scale. While the mean observed signals are relatively small, the long observational period allowed for identification of the following patterns for the observational period (April–September):

1. For liquid and mixed-phase clouds, liquid effective radius r_e is reduced in the Prudhoe Bay by up to 1.0 μm when averaging over the full data set (Figure 3). When limiting the data to easterly winds, the main wind direction, the reduction increases to up to 1.35 μm. For individual cases, the reduction in r_e can be larger (Figure 2)
2. For cloud frequency of occurrence (CFO) and liquid water path (LWP), pronounced regional gradients in CFO and LWP overlay potential local effects centered on the Prudhoe Bay area (Figures 4a and 4b). If there were such effects, they must be smaller than approximately 2 percentage points and 5 g $^{-2}$m for CFO and LWP, respectively
3. In combination, these anthropogenic aerosol impacts on cloud properties are estimated to result in a mean increase of upwelling shortwave radiation ($\Delta SW_{\uparrow}$) of up to 0.79 Wm^{-2} for the April–September period (Figure 4c)

Despite the challenging conditions for MODIS retrievals for land pixels at high latitudes due to low solar zenith angles and bright surfaces (Grosvenor & Wood, 2014; King et al., 2004; Platnick et al., 2001), we found our results to be robust with respect to the applied filters and retrieval methods. Our findings are consistent with the theory of aerosol cloud interaction that enhanced CCN concentrations modify cloud

properties. Reduced cloud droplet sizes associated with elevated CCN concentrations are notable in the MODIS observations, but the question as to whether there is a small change in CFO or LWP related to localized pollution could not be answered with the available data and is left open for future studies. Answering this question is crucial to fully quantify the impact of localized pollution on the radiative budget. The found changes in r_e and $\Delta SW_{\uparrow}$ are small in comparison to those often observed for ship tracks (e.g., up to 4.1 μm according to Christensen & Stephens, 2011) but localized emissions do—unlike ships—not move so that even small r_e can be locally highly relevant over time. In general, the exact value of the cloud response depends strongly on the methodological approach. This includes the question whether the polluted plume boundaries are well identified and compared with its pristine surroundings (Christensen & Stephens, 2011; Goren & Rosenfeld, 2014), and whether a climatological mean is estimated (Christensen & Stephens, 2011; Diamond et al., 2020) rather than an instantaneous effects (Goren & Rosenfeld, 2012, 2014). For instance, a case study approach focusing on well defined ship tracks showed a negative cloud radiative effect (CRE) of 4 W m^{-2} for ship tracks embedded within closed cells (Goren & Rosenfeld, 2014). In contrast, Diamond et al. (2020) provides a climatological estimate of −2 W m^{-2} due to cloud brightening within the southeast Atlantic shipping corridor.

It is important to note that the current approach likely underestimates the total impact on cloud radiative forcing because (a) optically thin clouds are not considered due to instrument limitations and (b) we use a surface estimate for $SW_{\downarrow}$ from CERES which is slightly more attenuated than the relevant $SW_{\downarrow}$ at cloud top (McCoy & Hartmann, 2015). Our $\Delta SW_{\uparrow}$ estimate is based only on r_e change and does not account for potential LWP adjustments. A full assessment of the radiative impact is important to understanding the net impacts of industrial activities on the surface energy budget, ice and snow formation and melt, the subsequent controls imparted on terrestrial ecosystems, and the associated feedback mechanisms. Our $\Delta SW_{\uparrow}$ estimate is only applicable to the period covered by observations (April–September) and needs to be reduced by approximately 50% to be representative for a full year.

This study gives a first estimate on the types of cloud perturbations that might be possible in the future in other industrialized regions of the Arctic. In a future warmer, more easily accessible Arctic, industrial activities are expected to increase which is potentially leading to rising local-source aerosol concentrations. Assuming that industrial emissions related to oil extraction produce higher emission than other anthropogenic activities in the Arctic, this study provides an upper boundary for microphysical and radiative effects related to localized pollution. Additional work is required to fully understand the impact of localized pollution on the ice phase of liquid containing clouds. This includes developing methods to reduce the uncertainties of space-based cloud retrievals for optically thin clouds and analyzing data of the ground-based observations of the Department of Energy Atmospheric Radiation Measurement (DOE ARM) sites in Alaska.

Acknowledgments
This work was supported by the US Department of Energy (DOE) Atmospheric System Research (ASR) program (DE-SC0013306) and the National Oceanic and Atmospheric Administration (NOAA) Physical Sciences Laboratory (PSL). We gratefully acknowledge the funding by the Deutsche Forschungsgemeinschaft (DFG, German Research Foundation) for the "Arctic Amplification: Climate Relevant Atmospheric and Surface Processes, and Feedback Mechanisms" (AC)[3] Project 268020496–TRR 172 within the Transregional Collaborative Research Center. T. G. acknowledges funding by the European Union via its Horizon 2020 project FORCeS (GA 821205) and by the DFG project CDNC4ACI (GZ QU 311/27-1). This study contains modified Copernicus Climate Change Service information (Copernicus Climate Change Service (C3S), 2017). Neither the European Commission nor ECMWF is responsible for any use that may be made of the Copernicus Information or Data it contains.
Open access funding enabled and organized by Projekt DEAL.

Data Availability Statement

Datasets: MODIS data products (MOD06L2, MYD06L2, collection 6, Platnick & Ackerman, 2015a; Platnick & Ackerman, 2015b) are available at https://ladsweb.modaps.eosdis.nasa.gov/missions-and-measurements/products/MOD06_gL2/ and https://ladsweb.modaps.eosdis.nasa.gov/missions-and-measurements/products/MYD06_gL2/, respectively; IMS Daily Northern Hemisphere Snow and Ice Analysis at 4 km resolution (National Ice Center, 2008, updated daily) can be retrieved at https://nsidc.org/data/G02156/versions/1; the repository of the ARM-standard Meteorological Instrumentation at Surface (MET, Holdridge & Kyrouac, 1993) is at https://www.archive.arm.gov/discovery/#v/results/s/fdsc::met; ERA5 hourly data on pressure levels from 1979 to present (Copernicus Climate Change Service (C3S), 2017) is available at https://cds.climate.copernicus.eu/cdsapp#!/dataset/10.24381/cds.bd0915c6.

References

Albrecht, B. A. (1989). Aerosols, cloud microphysics, and fractional cloudiness. *Science*, *245*(4923), 1227–1230. https://doi.org/10.1126/science.245.4923.1227

Borys, R. D., Lowenthal, D. H., Cohn, S. A., & Brown, W. O. J. (2003). Mountaintop and radar measurements of anthropogenic aerosol effects on snow growth and snowfall rate. *Geophysical Research Letters*, *30*(10), 1538. https://doi.org/10.1029/2002GL016855

Charlson, R. J., Schwartz, S. E., Hales, J. M., Cess, R. D., Coakley, J. A., Hansen, J. E., & Hofmann, D. J. (1992). Climate forcing by anthropogenic aerosols. *Science*, *255*(5043), 423–430. https://doi.org/10.1126/science.255.5043.423

Christensen, M. W., & Stephens, G. L. (2011). Microphysical and macrophysical responses of marine stratocumulus polluted by underlying ships: Evidence of cloud deepening. *Journal of Geophysical Research*, *116*(D3), D03201. https://doi.org/10.1029/2010JD014638
Coopman, Q., Garrett, T. J., Finch, D. P., & Riedi, J. (2018). High sensitivity of Arctic liquid clouds to long-range anthropogenic aerosol transport. *Geophysical Research Letters*, *45*(1), 372–381. https://doi.org/10.1002/2017GL075795
Copernicus Climate Change Service (C3S). (2017). *ERA5: Fifth generation of ECMWF atmospheric reanalyses of the global climate*. Copernicus Climate Change Service Climate Data Store (CDS). https://doi.org/10.24381/cds.bd0915c6
Creamean, J. M., Maahn, M., de Boer, G., McComiskey, A., Sedlacek, A. J., & Feng, Y. (2018). The influence of local oil exploration and regional wildfires on summer 2015 aerosol over the North Slope of Alaska. *Atmospheric Chemistry and Physics*, *18*(2), 555–570. https://doi.org/10.5194/acp-18-555-2018
de Boer, G., Eloranta, E. W., & Shupe, M. D. (2009). Arctic mixed-phase stratiform cloud properties from multiple years of surface-based measurements at two high-latitude locations. *Journal of the Atmospheric Sciences*, *66*(9), 2874–2887. https://doi.org/10.1175/2009JAS3029.1
de Boer, G., Morrison, H., Shupe, M. D., & Hildner, R. (2011). Evidence of liquid dependent ice nucleation in high-latitude stratiform clouds from surface remote sensors. *Geophysical Research Letters*, *38*(1), L01803. https://doi.org/10.1029/2010GL046016
Diamond, M. S., Director, H. M., Eastman, R., Possner, A., & Wood, R. (2020). Substantial cloud brightening from shipping in subtropical low clouds. *AGU Adv*, *1*(1), e2019AV000111. https://doi.org/10.1029/2019AV000111
Engelmann, R., Ansmann, A., Ohneiser, K., Griesche, H., Radenz, M., Hofer, J., et al. (2020). UTLS wildfire smoke over the North Pole region, Arctic haze, and aerosol-cloud interaction during MOSAiC 2019/20: An introductory. *Atmospheric Chemistry and Physics Discussions*, 1–41. https://doi.org/10.5194/acp-2020-1271
Feingold, G., McComiskey, A., Yamaguchi, T., Johnson, J. S., Carslaw, K. S., & Schmidt, K. S. (2016). New approaches to quantifying aerosol influence on the cloud radiative effect. *Proceedings of the National Academy of Sciences*, *113*(21), 5812–5819. https://doi.org/10.1073/pnas.1514035112
Garrett, T. J., & Zhao, C. (2006). Increased Arctic cloud longwave emissivity associated with pollution from mid-latitudes. *Nature*, *440*(7085), 787–789. https://doi.org/10.1038/nature04636
Gilgen, A., Huang, W. T. K., Ickes, L., Neubauer, D., & Lohmann, U. (2018). How important are future marine and shipping aerosol emissions in a warming Arctic summer and autumn? *Atmospheric Chemistry and Physics*, *18*(14), 10521–10555. https://doi.org/10.5194/acp-18-10521-2018
Goren, T., & Rosenfeld, D. (2012). Satellite observations of ship emission induced transitions from broken to closed cell marine stratocumulus over large areas. *Journal of Geophysical Research*, *117*, D17206. https://doi.org/10.1029/2012JD017981
Goren, T., & Rosenfeld, D. (2014). Decomposing aerosol cloud radiative effects into cloud cover, liquid water path and Twomey components in marine stratocumulus. *Atmospheric Research*, *138*, 378–393. https://doi.org/10.1016/j.atmosres.2013.12.008
Goren, T., Rosenfeld, D., Sourdeval, O., & Quaas, J. (2018). Satellite observations of precipitating marine stratocumulus show greater cloud fraction for decoupled clouds in comparison to coupled clouds. *Geophysical Research Letters*, *45*(10), 5126–5134. https://doi.org/10.1029/2018GL078122
Grandey, B. S., & Wang, C. (2019). Background conditions influence the estimated cloud radiative effects of anthropogenic aerosol emissions from different source regions. *Journal of Geophysical Research: Atmospheres*, *124*(4), 2276–2295. https://doi.org/10.1029/2018JD029644
Grosvenor, D. P., & Wood, R. (2014). The effect of solar zenith angle on MODIS cloud optical and microphysical retrievals within marine liquid water clouds. *Atmospheric Chemistry and Physics*, *14*(14), 7291–7321. https://doi.org/10.5194/acp-14-7291-2014
Gryspeerdt, E., Goren, T., & Smith, T. W. P. (2021). Observing the timescales of aerosol–cloud interactions in snapshot satellite images. *Atmospheric Chemistry and Physics*, *21*(8), 6093–6109. https://doi.org/10.5194/acp-21-6093-2021
Gryspeerdt, E., Goren, T., Sourdeval, O., Quaas, J., Mülmenstädt, J., Dipu, S., et al. (2019). Constraining the aerosol influence on cloud liquid water path. *Atmospheric Chemistry and Physics*, *19*(8), 5331–5347. https://doi.org/10.5194/acp-19-5331-2019
Gryspeerdt, E., Quaas, J., & Bellouin, N. (2016). Constraining the aerosol influence on cloud fraction. *Journal of Geophysical Research: Atmospheres*, *121*(7), 3566–3583. https://doi.org/10.1002/2015JD023744
Hallett, J., & Mossop, S. C. (1974). Production of secondary ice particles during the riming process. *Nature*, *249*(5452), 26–28. https://doi.org/10.1038/249026a0
Helfrich, S. R., McNamara, D., Ramsay, B. H., Baldwin, T., & Kasheta, T. (2007). Enhancements to and forthcoming developments in the Interactive Multisensor Snow and Ice Mapping System (IMS). *Hydrological Processes*, *21*(12), 1576–1586. https://doi.org/10.1002/hyp.6720
Hobbs, P. V., & Rangno, A. L. (1998). Microstructures of low and middle-level clouds over the Beaufort Sea. *Quarterly Journal of the Royal Meteorological Society*, *124*(550), 2035–2071. https://doi.org/10.1002/qj.49712455012
Holdridge, D., & Kyrouac, J. (1993). *ARM-standard meteorological instrumentation at surface (MET). Atmospheric radiation measurement (ARM) archive, oak ridge national laboratory (ORNL)*. https://doi.org/10.5439/1025220
Khanal, S., Wang, Z., & French, J. R. (2020). Improving middle and high latitude cloud liquid water path measurements from MODIS. *Atmospheric Research*, *243*, n. https://doi.org/10.1016/j.atmosres.2020.105033
King, M. D., Platnick, S., Yang, P., Arnold, G. T., Gray, M. A., Riedi, J. C., et al. (2004). Remote sensing of liquid water and ice cloud optical thickness and effective radius in the Arctic: Application of airborne multispectral MAS data. *Journal of Atmospheric and Oceanic Technology*, *21*(6), 857–875. https://doi.org/10.1175/1520-0426(2004)021⟨0857:RSOLWA⟩2.0.CO;2
Klein, S. A., McCoy, R. B., Morrison, H., Ackerman, A. S., Avramov, A., de Boer, G., et al. (2009). Intercomparison of model simulations of mixed-phase clouds observed during the ARM Mixed-Phase Arctic Cloud Experiment. I: Single-layer cloud. *Quarterly Journal of the Royal Meteorological Society*, *135*(641), 979–1002. https://doi.org/10.1002/qj.416
Klimont, Z., Kupiainen, K., Heyes, C., Purohit, P., Cofala, J., Rafaj, P., et al. (2017). Global anthropogenic emissions of particulate matter including black carbon. *Atmospheric Chemistry and Physics*, *17*(14), 8681–8723. https://doi.org/10.5194/acp-17-8681-2017
Kolesar, K. R., Cellini, J., Peterson, P. K., Jefferson, A., Tuch, T., Birmili, W., et al. (2017). Effect of Prudhoe Bay emissions on atmospheric aerosol growth events observed in Utqiaġvik (Barrow), Alaska. *Atmospheric Environment*, *152*, 146–155. https://doi.org/10.1016/j.atmosenv.2016.12.019
Korolev, A. (2007). Limitations of the Wegener–Bergeron–Findeisen mechanism in the evolution of mixed-phase clouds. *Journal of the Atmospheric Sciences*, *64*(9), 3372–3375. https://doi.org/10.1175/JAS4035.1
Korolev, A., McFarquhar, G., Field, P. R., Franklin, C., Lawson, P., Wang, Z., et al. (2017). Mixed-phase clouds: Progress and challenges. *Meteorological Monographs*, *58*, 5–15. https://doi.org/10.1175/AMSMONOGRAPHS-D-17-0001.1
Lacis, A. A., & Hansen, J. (1974). A parameterization for the absorption of solar radiation in the earth's atmosphere. *Journal of the Atmospheric Sciences*, *31*(1), 118–133. https://doi.org/10.1175/1520-0469(1974)031⟨0118:APFTAO⟩2.0.CO;2
Lance, S., Shupe, M. D., Feingold, G., Brock, C. A., Cozic, J., Holloway, J. S., et al. (2011). Cloud condensation nuclei as a modulator of ice processes in Arctic mixed-phase clouds. *Atmospheric Chemistry and Physics*, *11*(15), 8003–8015. https://doi.org/10.5194/acp-11-8003-2011

Lohmann, U. (2002). A glaciation indirect aerosol effect caused by soot aerosols. *Geophysical Research Letters*, *29*(4), 2002. https://doi.org/10.1029/2001GL014357

Lubin, D., & Vogelmann, A. M. (2006). A climatologically significant aerosol longwave indirect effect in the Arctic. *Nature*, *439*(7075), 453–456. https://doi.org/10.1038/nature04449

Maahn, M., de Boer, G., Creamean, J. M., Feingold, G., McFarquhar, G. M., Wu, W., & Mei, F. (2017). The observed influence of local anthropogenic pollution on northern Alaskan cloud properties. *Atmospheric Chemistry and Physics*, *17*(23), 14709–14726. https://doi.org/10.5194/acp-17-14709-2017

Maddux, B. C., Ackerman, S. A., & Platnick, S. (2010). Viewing geometry dependencies in MODIS cloud products. *Journal of Atmospheric and Oceanic Technology*, *27*(9), 1519–1528. https://doi.org/10.1175/2010JTECHA1432.1

Malavelle, F. F., Haywood, J. M., Jones, A., Gettelman, A., Clarisse, L., Bauduin, S., et al. (2017). Strong constraints on aerosol–cloud interactions from volcanic eruptions. *Nature*, *546*(7659), 485–491. https://doi.org/10.1038/nature22974

McCoy, D. T., & Hartmann, D. L. (2015). Observations of a substantial cloud-aerosol indirect effect during the 2014-2015 Bárðarbunga-Veiðivötn fissure eruption in Iceland. *Geophysical Research Letters*, *42*(23), 10409–10414. https://doi.org/10.1002/2015GL067070

Meskhidze, N., & Nenes, A. (2006). Phytoplankton and cloudiness in the Southern Ocean. *Science*, *314*(5804), 1419–1423. https://doi.org/10.1126/science.1131779

Morrison, H., de Boer, G., Feingold, G., Harrington, J., Shupe, M. D., & Sulia, K. (2012). Resilience of persistent Arctic mixed-phase clouds. *Nature Geoscience*, *5*(1), 11–17. https://doi.org/10.1038/ngeo1332

Morrison, H., Shupe, M. D., Pinto, J. O., & Curry, J. A. (2005). Possible roles of ice nucleation mode and ice nuclei depletion in the extended lifetime of Arctic mixed-phase clouds. *Geophysical Research Letters*, *32*(18), L18801. https://doi.org/10.1029/2005GL023614

National Ice Center. (2008). *IMS daily northern hemisphere snow and ice analysis at 4 km resolution. Version 1*. NSIDC: National Snow and Ice Data Center. updated daily. https://doi.org/10.7265/N52R3PMC

Norgren, M. S., de Boer, G., & Shupe, M. D. (2018). Observed aerosol suppression of cloud ice in low-level Arctic mixed-phase clouds. *Atmospheric Chemistry and Physics*, *18*(18), 13345–13361. https://doi.org/10.5194/acp-18-13345-2018

Platnick, S., & Ackerman, S. (2015). *MODIS/Aqua Atmosphere L2 Cloud Product (06_L2). NASA MODIS Adaptive Processing System, Goddard Space Flight Center, USA*. NASA Level 1 and Atmosphere Archive and Distribution System. https://doi.org/10.5067/MODIS/MYD06_gL2.006

Platnick, S., & Ackerman, S. (2015). *MODIS/Terra Atmosphere L2 Cloud Product (06_L2). NASA MODIS Adaptive Processing System, Goddard Space Flight Center, USA*. Level 1 and Atmosphere Archive and Distribution System (LAADS). https://doi.org/10.5067/MODIS/MOD06_gL2.006

Platnick, S., Li, J. Y., King, M. D., Gerber, H., & Hobbs, P. V. (2001). A solar reflectance method for retrieving the optical thickness and droplet size of liquid water clouds over snow and ice surfaces. *Journal of Geophysical Research*, *106*(D14), 15185–15199. https://doi.org/10.1029/2000JD900441

Platnick, S., & Twomey, S. (1994). Remote sensing the susceptibility of cloud albedo to changes in drop concentration. *Atmospheric Research*, *34*(1), 85–98. https://doi.org/10.1016/0169-8095(94)90082-5

Possner, A., Ekman, A. M. L., & Lohmann, U. (2017). Cloud response and feedback processes in stratiform mixed-phase clouds perturbed by ship exhaust. *Geophysical Research Letters*, *44*, 1964–1972. https://doi.org/10.1002/2016GL071358

Quaas, J., Arola, A., Cairns, B., Christensen, M., Deneke, H., Ekman, A. M. L., et al. (2020). Constraining the Twomey effect from satellite observations: Issues and perspectives. *Atmospheric Chemistry and Physics*, *20*(23), 15079–15099. https://doi.org/10.5194/acp-20-15079-2020

Quinn, P. K., Bates, T. S., Schulz, K., & Shaw, G. E. (2009). Decadal trends in aerosol chemical composition at Barrow, Alaska: 1976–2008. *Atmospheric Chemistry and Physics*, *9*(22), 8883–8888. https://doi.org/10.5194/acp-9-8883-2009

Ramsay, B. H. (1998). The interactive multisensor snow and ice mapping system. *Hydrological Processes*, *12*, 1537–1546. https://doi.org/10.1002/(SICI)1099-1085(199808/09)12:10/11⟨1537::AID-HYP679⟩3.3.CO;2

Rangno, A. L., & Hobbs, P. V. (2001). Ice particles in stratiform clouds in the Arctic and possible mechanisms for the production of high ice concentrations. *Journal of Geophysical Research*, *106*(D14), 15065–15075. https://doi.org/10.1029/2000JD900286

Rosenfeld, D., Zhu, Y., Wang, M., Zheng, Y., Goren, T., & Yu, S. (2019). Aerosol-driven droplet concentrations dominate coverage and water of oceanic low level clouds. *Science*, *363*, eaav0566. https://doi.org/10.1126/science.aav0566

Schmale, J., Zieger, P., & Ekman, A. M. L. (2021). Aerosols in current and future Arctic climate. *Nature Climate Change*, *11*(2), 95–105. https://doi.org/10.1038/s41558-020-00969-5

Sedlar, J., Igel, A., & Telg, H. (2021). Processes contributing to cloud dissipation and formation events on the North Slope of Alaska. *Atmospheric Chemistry and Physics*, *21*(5), 4149–4167. https://doi.org/10.5194/acp-21-4149-2021

Sena, E. T., McComiskey, A., & Feingold, G. (2016). A long-term study of aerosol–cloud interactions and their radiative effect at the Southern Great Plains using ground-based measurements. *Atmospheric Chemistry and Physics*, *16*(17), 11301–11318. https://doi.org/10.5194/acp-16-11301-2016

Shupe, M. D. (2011). Clouds at Arctic atmospheric observatories. part II: Thermodynamic phase characteristics. *Journal of Applied Meteorology and Climatology*, *50*(3), 645–661. https://doi.org/10.1175/2010JAMC2468.1

Shupe, M. D., & Intrieri, J. M. (2004). Cloud radiative forcing of the Arctic surface: The influence of cloud properties, surface albedo, and solar zenith angle. *Journal of Climate*, *17*(3), 616–628. https://doi.org/10.1175/1520-0442(2004)017⟨0616:CRFOTA⟩2.0.CO;2

Shupe, M. D., Uttal, T., & Matrosov, S. Y. (2005). Arctic cloud microphysics retrievals from surface-based remote sensors at SHEBA. *Journal of Applied Meteorology*, *44*(10), 1544–1562. https://doi.org/10.1175/JAM2297.1

Solomon, A., de Boer, G., Creamean, J. M., McComiskey, A., Shupe, M. D., Maahn, M., & Cox, C. (2018). The relative impact of cloud condensation nuclei and ice nucleating particle concentrations on phase partitioning in Arctic mixed-phase stratocumulus clouds. *Atmospheric Chemistry and Physics*, *18*(23), 17047–17059. https://doi.org/10.5194/acp-18-17047-2018

Sourdeval, O., Labonnote, C. L., Baran, A. J., & Brogniez, G. (2015). A methodology for simultaneous retrieval of ice and liquid water cloud properties. Part I: Information content and case study. *Quarterly Journal of the Royal Meteorological Society*, *141*(688), 870–882. https://doi.org/10.1002/qj.2405

Stephens, G. L. (2005). Cloud feedbacks in the climate system: A critical review. *Journal of Climate*, *18*(2), 237–273. https://doi.org/10.1175/JCLI-3243.1

Stevens, B., & Feingold, G. (2009). Untangling aerosol effects on clouds and precipitation in a buffered system. *Nature*, *461*(7264), 607–613. https://doi.org/10.1038/nature08281

Sulia, K. J., & Harrington, J. Y. (2011). Ice aspect ratio influences on mixed-phase clouds: Impacts on phase partitioning in parcel models. *Journal of Geophysical Research*, *116*(D21), D21309. https://doi.org/10.1029/2011JD016298

Toll, V., Christensen, M., Quaas, J., & Bellouin, N. (2019). Weak average liquid-cloud-water response to anthropogenic aerosols. *Nature*, *572*(7767), 51–55. https://doi.org/10.1038/s41586-019-1423-9

Trofimov, H., Bellouin, N., & Toll, V. (2020). Large-scale industrial cloud perturbations confirm bidirectional cloud water responses to anthropogenic aerosols. *Journal of Geophysical Research: Atmospheres*, *125*(14), e2020JD032575. https://doi.org/10.1029/2020JD032575

Twomey, S. (1976). The effects of fluctuations in liquid water content on the evolution of large drops by coalescence. *Journal of the Atmospheric Sciences*, *33*(4), 720–723. https://doi.org/10.1175/1520-0469(1976)033⟨0720:TEOFIL⟩2.0.CO;2

Wood, R. (2007). Cancellation of aerosol indirect effects in marine stratocumulus through cloud thinning. *Journal of the Atmospheric Sciences*, *64*(7), 2657–2669. https://doi.org/10.1175/JAS3942.1

Yang, F., Ovchinnikov, M., & Shaw, R. A. (2015). Long-lifetime ice particles in mixed-phase stratiform clouds: Quasi-steady and recycled growth. *Journal of Geophysical Research: Atmospheres*, *120*(22), 11617–11635. https://doi.org/10.1002/2015JD023679

Zamora, L. M., Kahn, R. A., Eckhardt, S., McComiskey, A., Sawamura, P., Moore, R., & Stohl, A. (2017). Aerosol indirect effects on the nighttime Arctic Ocean surface from thin, predominantly liquid clouds. *Atmospheric Chemistry and Physics*, *17*(12), 7311–7332. https://doi.org/10.5194/acp-17-7311-2017

Zamora, L. M., Kahn, R. A., Huebert, K. B., Stohl, A., & Eckhardt, S. (2018). A satellite-based estimate of combustion aerosol cloud microphysical effects over the Arctic Ocean. *Atmospheric Chemistry and Physics*, *18*(20), 14949–14964. https://doi.org/10.5194/acp-18-14949-2018